Polycarbon Disulfides SC_nS (n = 1−3) and Their Protonated and Methylated Forms ($HC_nS_2^+$ and $CH_3C_nS_2^+$): Tandem Mass Spectrometry and ab Initio MO Study

Ming Wah Wong,*,† Curt Wentrup,*,† and Robert Flammang*,‡

Department of Chemistry, The University of Queensland, Brisbane QLD 4072, Australia, and Organic Chemistry Laboratory, University of Mons-Hainaut, 19 Avenue Maistriau, B-7000 Mons, Belgium

Received: July 11, 1995; In Final Form: September 5, 1995®

Dissociative ionization of 4,5-bis(methylthio)-1,2-dithiole-3-thione (**1**) has allowed the detection of a series of carbon disulfide radical cations, $SC_nS^{\bullet+}$ (n = 1−3), and their *S*-methylated forms, $CH_3SC_nS^+$, in the gas phase of a mass spectrometer. The connectivities and stabilities of these ions and the corresponding neutrals have been probed by collisional activation (CA) and neutralization−reionization (NR) mass spectrometry. Moreover, the sites of protonation and cationic methylation of the polycarbon disulfides have been investigated by a combination of flash vacuum pyrolysis, chemical ionization, and CAMS (FVP/CI/MS/MS). The experimental results are supported by ab initio MO calculations at the QCISD(T)/6-311+G(2d,p) + ZPVE level. Both experiments and calculations indicate that the most favorable site of protonation and methylation is the carbon atom for C_2S_2 and C_3S_2 but a sulfur atom for CS_2. The proton affinities (298 K) of C_2S_2 and C_3S_2 are predicted to be 842 and 818 kJ mol^{-1}, respectively.

Introduction

In connection with our current interest in the production and identification of heterocumulenes X=(C)$_n$=Y (n = 2, 3) and their protonated forms (SCCS,[1] HNCCO,[2] HNCCS,[3] HNCCCO,[4] HNCCCS,[5] OCCHCO$^+$,[6] and HNCCHCO$^+$[7]), we wish to report a series of $SC_nS^{\bullet+}$, $[SC_nS]H^+$, and $[SC_nS]CH_3^+$ ions (n = 1−3).[8] We have determined their atom connectivities by collisional activation (CA)[9] and evaluated the gas-phase stabilities of the corresponding neutrals by neutralization−reionization (NR)[10] mass spectrometry. In addition, we determine the most favorable sites of protonation (methylation) in polycarbon disulfides using a combination of flash vacuum pyrolysis, chemical ionization, and CAMS (FVP/CI/MS/MS). The experimental characterization of the neutrals and cations is strongly supported by high-level ab initio molecular orbital calculations. The interplay between theory and experiment is particularly important for these short-lived species.[2−7] Theory can provide detailed information on the structures, energetics, and fragmentation patterns, which can be directly compared with experiment.

Experimental Section

The electron ionization (EI), collisional activation (CA), and neutralization−reionization (NR) mass spectra were recorded on a large-scale tandem mass spectrometer combining six sectors (VG AutoSpec 6F, VG Analytical, Manchester, U.K.) of $E_1B_1E_2E_3B_2E_4$ geometry (E stands for electric sector; B for magnetic sector).[11] The samples were introduced into the ion source *via* a direct insertion probe and ionized using the following source conditions: 70 eV ionizing electron energy, 200 μA trap current, 8 kV accelerating voltage, and 200 °C ion source temperature.

In the CA experiments, a beam of fast ions (8 keV) is mass-selected using the first three sectors at a mass resolution eliminating any possible interference with isobaric ions and then is subjected to collisional activation, usually with O_2 (80% transmittance). Some spectra were also obtained using He as the collision gas. Usually, there is no significant effect of the gas except that O_2 produces stronger charge-stripping peaks (compare *m/z* 50.5 in Figures 9C and 10). In the NR experiments, neutralization of the ions with CH_3OH or NH_3 (80% transmittance) precedes reionization with O_2 (also 80% T). Non-neutralized ions remaining after neutralization were eliminated by floating the calibration ion source inserted between the two cells at 9 kV. The spectra were recorded by scanning E_3 and collecting the ions in the fifth field free region.

In the FVP/MS/MS experiments, samples were vaporized through an electrically heated quartz tube (5 cm length, 3 mm width) installed in the source housing.[11b] CI experiments were carried out using CH_3I or CH_3Cl as a methylating agent and methane (CH_5^+) as the protonating agent.

Compounds **1**,[12,13] **3**,[12,13] **5**,[1] and **7**[14] were prepared according to the literature.

Computational Details

Standard ab initio molecular orbital calculations[15] were carried out with the GAUSSIAN 92[16] system of programs. Geometry optimizations were performed with the standard polarized split-valence 6-31G* basis set[15] at the Hartree−Fock (HF) and second-order Møller−Plesset perturbation levels.[15] Improved relative energies were obtained through quadratic configuration interaction with singles, doubles, and augmented triples (QCISD(T))[17] calculations with the larger 6-311+G(2d,p)[15] basis set, based on the MP2/6-31G* optimized geometries. This level of theory is evaluated with the use of the additivity approximation[15]

$$E(\text{QCISD(T)/6-311+G(2d,p)}) \approx E(\text{QCISD(T)/6-31G*}) - E(\text{MP2/6-31G*}) + E(\text{MP2/6-311+G(2d,p)}) \quad (1)$$

Our best relative energies discussed within the text correspond to QCISD/6-311+G(2d,p) values with zero-point contributions, computed from HF/6-31G* vibrational frequencies (scaled by 0.9135).[18] Spin-restricted calculations were used for closed-shell systems, and spin-unrestricted ones, for open-shell systems. The open-shell singlet state of C_2S_2 was calculated using the UHF formalism. The frozen-core approximation was employed for all correlated calculations.

† The University of Queensland.
‡ University of Mons-Hainaut.
® Abstract published in *Advance ACS Abstracts*, October 15, 1995.

0022-3654/95/2099-16849$09.00/0

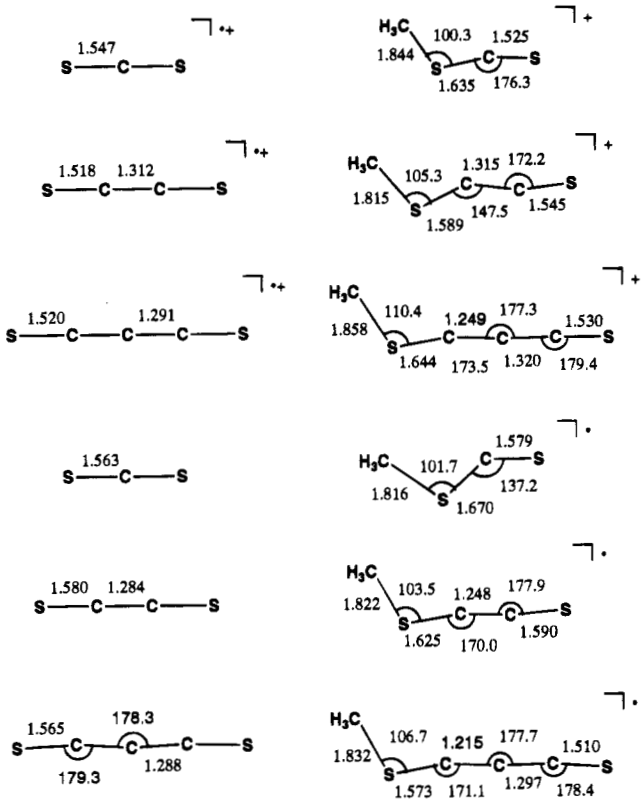

Figure 1. Optimized geometries (MP2/6-31G*) of $SC_nS^{\bullet+}$, SC_nS, $CH_3SC_nS^+$, and $CH_3SC_nS^\bullet$; bond lengths in angstroms and bond angles in degrees.

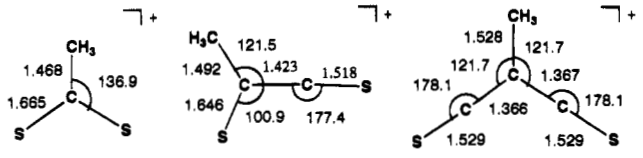

Figure 2. Optimized geometries (MP2/6-31G*) of *C*-methylated SC_nS ions; bond lengths in angstroms and bond angles in degrees.

The full set of optimized (MP2/6-31G*) equilibrium structures for $SC_nS^{\bullet+}$, SC_nS, $CH_3(SC_nS)^+$, and $CH_3SC_nS^\bullet$ is shown in Figures 1 and 2, and the calculated relative energies are summarized in Tables 1−3.

Results and Discussion

Fragmentation of the Radical Cations of 1,2-Dithiole-3-thione ($1^{\bullet+}$) and Dithietane ($3^{\bullet+}$). We have used 4,5-bis(methylthio)-1,2-dithiole-3-thione (**1**) as a convenient precursor of C_nS_2 ions. It has been demonstrated that, on treatment with phosphites, **1** is converted to 1,3-dithietane **3**[12] rather than the isomeric 3,3′-bi(1,2-dithiolylidene) **2**, as had been assumed previously (Scheme 1).[19] Dithietane **3** is formally a [2 + 2] dimer of thioacylthioketene **4**, which in turn is produced by flash vacuum pyrolysis (FVP) of **3** and identified by low-temperature IR spectroscopy in an argon matrix (17 K, 1746 cm^{-1}).[13] The FVP of **3** also produces significant amounts of CS_2, C_3S_2, and bis(methylthio)acetylene and is thus a convenient source of these molecules for mass spectrometric purposes. Electron ionization mass spectra (EIMS) of some 1,2-dithiole-3-thiones were recently reported.[20]

The EI mass spectrum of dithietane **3** features only a small peak at *m/z* 194 (6%) at a sample inlet temperature of 200 °C (base peak *m/z* 115 (100%), *m/z* 388 ($M^{\bullet+}$, 55%)). On FVP of **3** at 680 °C, we find an increase in *m/z* 194 corresponding to thermal formation of thioacylthioketene **4** (*m/z* 194 (13%), *m/z* 388 ($M^{\bullet+}$, 5%), *m/z* 76 (100%)). The CAMS of *m/z* 194 features the following signals in order of abundance: *m/z* 115 > 179 > 100 > 147 > 91. There are no peaks at *m/z* 118 or *m/z* 76 (CS_2), thus indicating the open-chain structure **4** rather than the four-centered cyclic thiete-2-thione **4′**.

SCHEME 1

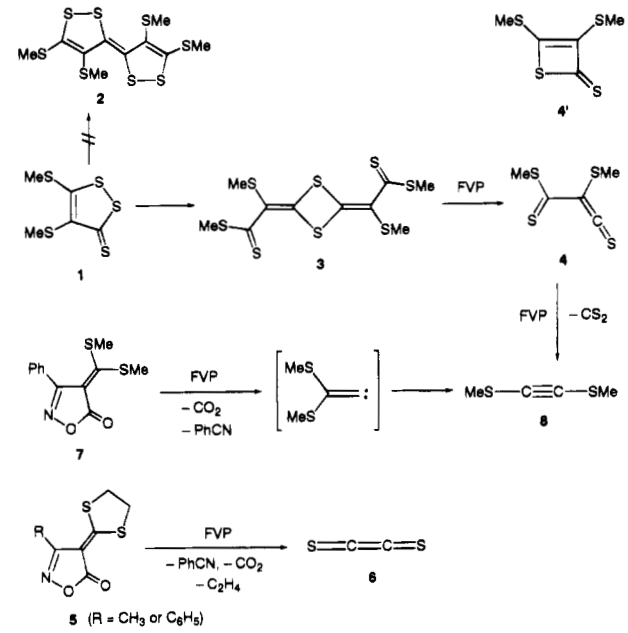

The EI mass spectrum of dithiolethione **1** features an intense parent peak at *m/z* 226 (Figure 3). Apart from the loss of $CH_3^\bullet$ (*m/z* 211), prominent fragment ion peaks are observed at *m/z* 147, 115, 103, 100, 91, 88, and 76. These ions, assigned the structures **a**−**g**, also dominate the CA mass spectrum of the molecular ions of **1**.

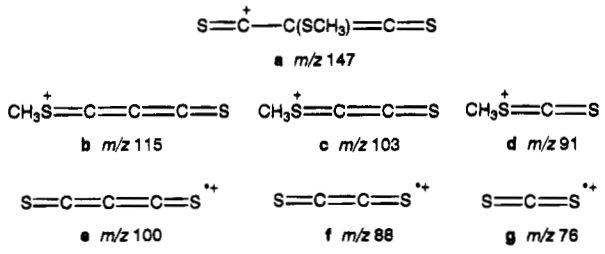

Resulting from consecutive losses of $CH_3^\bullet$ and S_2, the *m/z* 147 ions should have structure **a**. Their CA spectrum (Figure 4) features indeed an intense peak at *m/z* 100 (**e**) and a smaller one at *m/z* 103 (**c**), which can be readily explained on the basis of structure **a**. Loss of a methythio radical ($CH_3S^\bullet$) affords carbon subsulfide radical cations $SCCCS^{\bullet+}$ (**e**, *m/z* 100); this process, which is only observed if a collision gas (O_2) is present, is the lowest energy simple cleavage rection (Scheme 2). Consecutive losses of CS and $CH_3^\bullet$ are responsible for a third intense peak of interest and assigned to the ethenedithione ions $SCCS^{\bullet+}$ (**f**) (Scheme 2).

The calculated relative fragmentation energies of **a** (Table 1) are in good accord with the measured intensities in the CAMS except that the *m/z* 103 peak may be smaller than expected (Figure 4). In agreement with experiment, theory predicts that loss of $CH_3S^\bullet$ is the energetically most favorable fragmentation; **e** + $CH_3S^\bullet$ lies 277 kJ mol^{-1} above **a**. A similar value is calculated for the competitive loss of CS; **c** + CS lies 281 kJ mol^{-1} above **a**.

The connectivities SCCCS and SCCS for ions **e** and **f** are indicated by MS/MS/MS experiments. For example, Figure 5

TABLE 1: Calculated Fragmentation Energies[a] (kJ mol^{-1}) of $SC_nS^{\bullet+}$, $CH_3SC_nS^+$, and $SCC(SCH_3)CS^+$ Cations

$SCS^{\bullet+}$ (g)	
CS + $S^{\bullet+}$ (*m/z* 32)	615
S + $CS^{\bullet+}$ (*m/z* 44)	668
$SCCS^{\bullet+}$ (f)	
CS + $CS^{\bullet+}$ (*m/z* 44)	447
S + $CCS^{\bullet+}$ (*m/z* 56)	768
CCS + $S^{\bullet+}$ (*m/z* 32)	884
$SCCCS^{\bullet+}$ (e)	
CS + $CCS^{\bullet+}$ (*m/z* 56)	572
S + $CCCS^{\bullet+}$ (*m/z* 68)	697
CCS + $CS^{\bullet+}$ (*m/z* 44)	740
CCCS + $S^{\bullet+}$ (*m/z* 32)	744
CH_3SCCCS^+ (b)	
$CH_3^\bullet$ + $SCCCS^{\bullet+}$ (*m/z* 100)	259
SCCCS + CH_3^+ (*m/z* 15)	340
$CH_3CS^\bullet$ + $CCS^{\bullet+}$ (*m/z* 56)	340
$CH_3S^\bullet$ + $CCCS^{\bullet+}$ (*m/z* 68)	445
CCCS + CH_3S^+ (*m/z* 47)	563
CS + CH_3SCC^+ (*m/z* 71)	566
CCS + CH_3SC^+ (*m/z* 59)	725
$CH_3SCC^\bullet$ + $CS^{\bullet+}$ (*m/z* 44)	764
S + CH_3SCCC^+ (*m/z* 83)	769
$H^\bullet$ + $CH_2SCCC^{\bullet+}$ (*m/z* 114)	769
$CH_3SC^\bullet$ + $CCS^{\bullet+}$ (*m/z* 56)	851
CH_2SCCCS + H^+ (*m/z* 1)	890
$CH_3SCCC^\bullet$ + $S^{\bullet+}$ (*m/z* 32)	1065
CH_3SCS^+ (d)	
SCS + CH_3^+ (*m/z* 15)	293
$CH_3^\bullet$ + $SCS^{\bullet+}$ (*m/z* 76)	302
$H^\bullet$ + $CH_2SCS^{\bullet+}$ (*m/z* 90)	374
CS + CH_3S^+ (*m/z* 47)	477
$CH_3S^\bullet$ + $CS^{\bullet+}$ (*m/z* 44)	570
S + CH_3SC^+ (*m/z* 59)	695
CH_2SCS + H^+ (*m/z* 1)	861
$CH_3SC^\bullet$ + $S^{\bullet+}$ (*m/z* 32)	937
CH_3SCCS^+ (c)	
$CH_3^\bullet$ + $SCCS^{\bullet+}$ (*m/z* 88)	205
$H^\bullet$ + $CH_2SCCS^{\bullet+}$ (*m/z* 102)	363
CS + CH_3SC^+ (*m/z* 59)	378
SCCS + CH_3^+ (*m/z* 15)	387
$CH_3S^\bullet$ + $CCS^{\bullet+}$ (*m/z* 56)	574
CCS + CH_3S^+ (*m/z* 47)	649
$CH_3SC^\bullet$ + $CS^{\bullet+}$ (*m/z* 44)	673
S + CH_3SCC^+ (*m/z* 71)	708
CH_2SCCS + H^+ (*m/z* 1)	811
$CH_3SCC^\bullet$ + $S^{\bullet+}$ (*m/z* 32)	853
$SCC(SCH_3)CS^+$ (a)	
$CH_3S^\bullet$ + $SCCCS^{\bullet+}$ (*m/z* 100)	277
CS + CH_3SCCS^+ (*m/z* 103)	281
$CH_3^\bullet$ + $SCC(S)CS^{\bullet+}$ (*m/z* 132)	334
SCCCS + CH_3S^+ (*m/z* 47)	404
SCC(S)CS + CH_3^+ (*m/z* 15)	541
$CH_3SCCS^\bullet$ + $CS^{\bullet+}$ (*m/z* 44)	610

[a] QCISD(T)/6-311+G(2d,p) + ZPVE level.

TABLE 2: Calculated Fragmentation Energies[a] (kJ mol^{-1}) of SC_nS and $CH_3SC_nS^\bullet$ Neutrals

SCS		$CH_3SCS^\bullet$	
S (S) + CS (S)	536	$CH_3^\bullet$ + SCS	−1
S (T) + CS (T)	782	$CH_3S^\bullet$ + CS	136
		CH_2SCS + $H^\bullet$	195
SCCS (S)		$CH_3SC^\bullet$ + S	556
CS (S) + CS (S)	141		
S (T) + CCS (T)	481	$CH_3SCCS^\bullet$	
S (S) + CCS (S)	630	$CH_3^\bullet$ + SCCS	192
CS (T) + CS (T)	822	CH_2SCCS + $H^\bullet$	243
		$CH_3SC^\bullet$ + CS	337
SCCS (T)		$CH_3S^\bullet$ + CCS	407
CS (S) + CS (T)	495	$CH_3SCC^\bullet$ + S	570
S (T) + CCS (S)	548		
S (S) + CCS (T)	589	$CH_3SCCCS^\bullet$	
		$CH_3^\bullet$ + SCCS	−41
SCCCS		$CH_3S^\bullet$ + CCCS	134
CS (S) + CCS (S)	519	CH_2SCCCS + $H^\bullet$	136
S (S) + CCCS (S)	575	$CH_3SCC^\bullet$ + CS	242
S (T) + CCCS (T)	728	$CH_3SC^\bullet$ + CCS	498
CS (T) + CCS (T)	806	$CH_3SCCC^\bullet$ + S	505

[a] QCISD(T)/6-311+G(2d,p) + ZPVE level.

TABLE 3: Calculated *C*-Methylated SC_nS^+ Fragmentation Energies[a] (kJ mol)

$S(CH_3)CS^+$		$SC(CH_3)CS^+$ (i)	
SCS + CH_3^+ (*m/z* 15)	240	CS + CH_3CS^+ (*m/z* 59)	124
$CH_3^\bullet$ + $SCS^{\bullet+}$ (*m/z* 76)	249	$CH_3^\bullet$ + $SCCS^{\bullet+}$ (*m/z* 88)	289
S + CH_3CS^+ (*m/z* 59)	305	SCCS + CH_3^+ (*m/z* 15)	470
$CH_3CS^\bullet$ + $S^{\bullet+}$ (*m/z* 32)	706	S + CH_3CCS^+ (*m/z* 71)	566
		$CH_3CS^\bullet$ + $CS^{\bullet+}$ (*m/z* 44)	578
$SC(CH_3)CCS^+$ (k)		$CH_3CCS^\bullet$ + $S^{\bullet+}$ (*m/z* 32)	723
$CH_3^\bullet$ + $SCCCS^{\bullet+}$ (*m/z* 100)	340		
SCCCS + CH_3^+ (*m/z* 15)	420		
CS + CH_3CCS^+ (*m/z* 71)	421		
$CH_3CCS^\bullet$ + $CS^{\bullet+}$ (*m/z* 44)	630		

[a] QCISD(T)/6-311+G(2d,p) + ZPVE level.

shows the CA spectrum of mass-selected $C_3S_2^{\bullet+}$ (*m/z* 100) ions produced by collisional activation of *m/z* 147 ions. The intense peaks at *m/z* 68 ($CCCS^{\bullet+}$) and *m/z* 56 ($CCS^{\bullet+}$) and the identity of the CAMS with the spectrum obtained with an authentic sample of carbon subsulfide (vide infra) leave no doubt of the SCCCS connectivity.

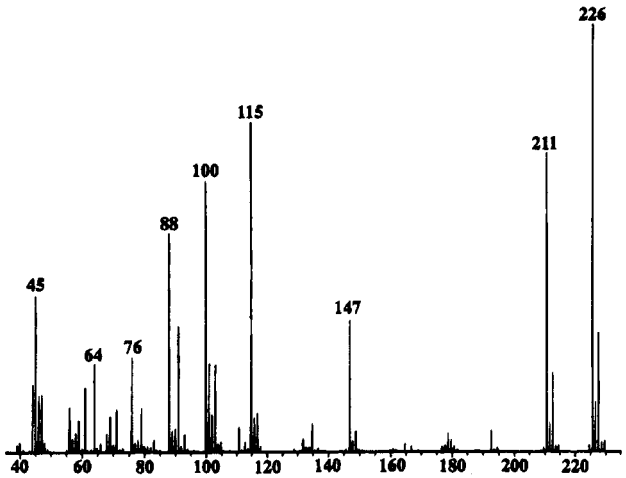

Figure 3. EI mass spectrum (70 eV) of 4,5-bis(methylthio)-1,2-dithiole-3-thione (1).

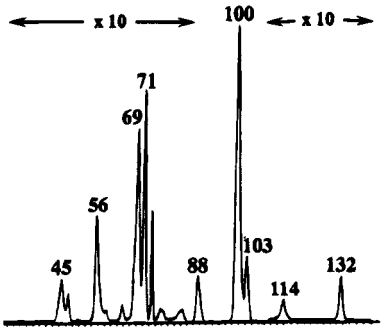

Figure 4. CA(O_2) spectrum of *m/z* 147 ions **a** from **1**.

For the *m/z* 103 ions **c**, the SCCS connectivity was again established by an MS/MS/MS experiment. Localization of CH_3 on sulfur is proposed on the basis of the structure of the precursor ions **a**; there is no favorable fragmentation process

TABLE 4: CA(O_2) Mass Spectra of $SC_nS^{\bullet+}$ Radical Cations[a]

species	precursor	88	76	68	64	56	50	44	38	36	32	24
$SCCS^{\bullet+}$	**1**	5	3	52	20	100	8[b]	15		2	10	<1
$SCCS^{\bullet+}$	**1**		6		4	39		100[b]			8	<1
$SCS^{\bullet+}$	**1**				16			100	11[b]		68	
$SCCCS^{\bullet+}$	**3**, FVP 680 °C	3	3	50	17	100	4	22		2	12	<1
$SCCS^{\bullet+}$	**5**, FVP 750 °C		5		2	36		100			3	<1
$SCS^{\bullet+}$	CS_2				18			100	7		71	

[a] Intensities expressed in percent relative to the most intense fragment ion peak. [b] Charge-stripping peaks (SC_nS^{2+} ions); superimposed for $SC_2S^{\bullet+}$ with $CS^{\bullet+}$ (estimated intensity of ca. 17%).

TABLE 5: NR (CH_3OH/O_2) Mass Spectra of $SC_nS^{\bullet+}$ Radical Cations[a]

species	*m/z*	100	88	76	68	64	56	50	44	38	36	32	24
$SCCS^{\bullet+}$		100	1	2	58	7	70	1	94		15	52	3
$SCCS^{\bullet+}$			69	2		2	31		100			30	1
$SCS^{\bullet+}$				100		3			49	<1		27	

[a] Intensities expressed in percent relative to the most intense ion peak.

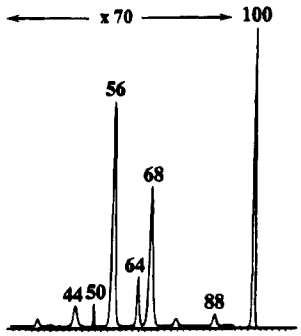

Figure 5. MS/MS/MS experiment: CA(O_2) mass spectrum of *m/z* 100 ions **e** produced by collisional activation (He) of mass-selected *m/z* 147 precursor ions.

SCHEME 2

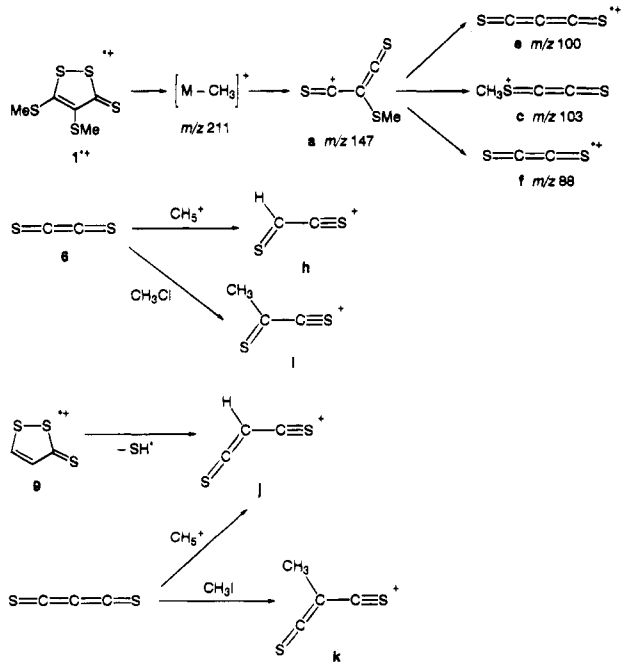

other than the loss of $CH_3^\bullet$ (Table 1). For distinguishing **c** and the *C*-methylated isomer **i**, see below.

Consecutive losses of $CH_3S^\bullet$ and S_2 from $\mathbf{1}^{\bullet+}$ produce abundant *m/z* 115 ions **b**. This behavior has already been noted for other 5-substituted 1,2-dithiole-3-thiones (losses of $H^\bullet$ + S_2)[21] and suggests that ions **b** incorporate the $CH_3S^\bullet$ group originating from position 5 in $\mathbf{1}^{\bullet+}$. The origin of ion **d** is less clear (it appears also in the CAMS and in the MIKE of $\mathbf{1}^{\bullet+}$); the loss of the $CH_3^\bullet$ group yields carbon disulfide ions (**g**). This fragmentation occurs in the MIKE spectrum and is strongly increased in the CA spectrum.

$SC_nS^{\bullet+}$ Radical Cations. The CA(O_2) mass spectra of the $SC_nS^{\bullet+}$ radical cations are collected in Table 4 and compared with the spectra of the reference ions. On-line coupling of flash vacuum pyrolysis (FVP) with the mass spectrometer allows the production and ionization of carbon subsulfide, S=C=C=C=S,[13] and ethenedithione, S=C=C=S (**6**),[1] starting from the dithietane **3** and 3-phenyl- or 3-methylisoxazolone derivatives **5** (Scheme 1), respectively. The identity of the spectra with those described above leaves no doubt as to the connectivities of ions **e**–**g** as produced from $\mathbf{1}^{\bullet+}$.[22] The CA mass spectra of $SCCS^{\bullet+}$ and $SCCCS^{\bullet+}$ also agree well with those reported by Schwarz and co-workers.[24]

All $SC_nS^{\bullet+}$ ions are calculated to be thermodynamically stable species in the gas phase (Table 1). The computed relative fragmentation energies are in excellent agreement with the observed CAMS (Table 4). Loss of CS represents the lowest energy fragmentation process in all cases. The $SC_nS^{\bullet+}$ ions are all predicted to possess a linear geometry. The C—C and C—S bond lengths of the $SCCS^{\bullet+}$ radical cations are significantly different from those of the corresponding neutrals (Figure 1). This may be rationalized by considering the effect of ionization of the S=C=C=S neutral. The highest occupied orbital (HOMO) of SCCS is C—C bonding but C—S antibonding. Removal of an electron from this antibonding π^* orbital would result in a longer C—C bond and shorter C—S bonds. The same conclusion is revealed by considering Lewis structures: the C_2S_2 radical cation can be regarded as the resonance hybrid $S{=}\dot{C}{-}C{\equiv}S^+ \leftrightarrow {}^+S{\equiv}C{-}\dot{C}{=}S$.

$CH_3SC_nS^+$ Cations. The CA(O_2) mass spectra of the methylated ions **b**–**d** are characterized by a very pronounced loss of $CH_3^\bullet$ (Figure 6). Loss of CS is another common reaction of ions **b**–**d**, leading to *m/z* 71, 59, and 47 ions, respectively.

The *S*-methylated ions (**b**–**d**) are also predicted to be observable species in the gas phase. The energetically most favorable fragmentation reactions correspond to the loss of $CH_3^\bullet$ and CS, again in good accord with the measured intensities in both CAMS and NRMS (see next section).[25] In contrast to $SC_nS^{\bullet+}$, the $CH_3SC_nS^+$ ions are calculated to have a bent SC_nS skeleton (Figure 1).

SC_nS Neutrals. As expected, the NR mass spectra of the $SC_nS^{\bullet+}$ radical cations (**e**–**g**) are characterized by very strong recovery signals corresponding to survivor ions (Table 5). As pointed out previously, structurally significant peaks are somewhat enhanced in NRMS compared to CAMS due to a higher

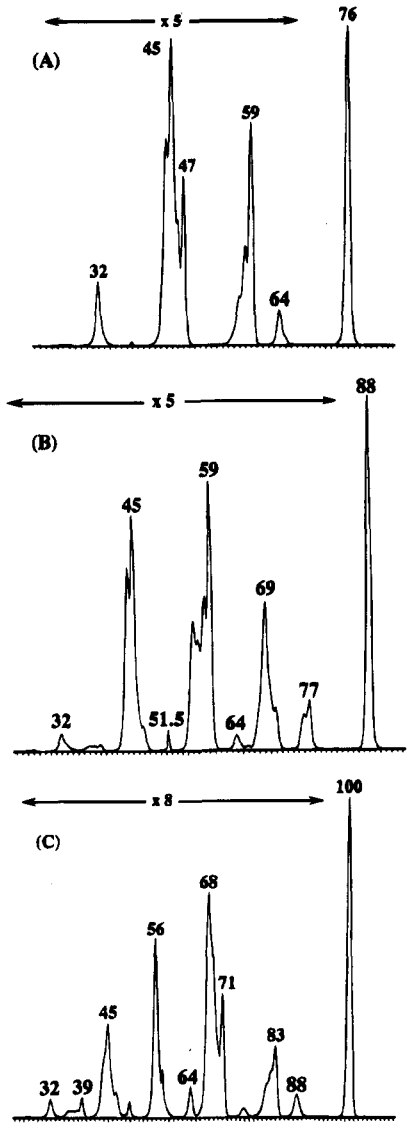

Figure 6. $CA(O_2)$ mass spectra of *S*-methylated ions **b**−**d** [*m/z* 91 (A), *m/z* 103 (B), and *m/z* 115 (C)].

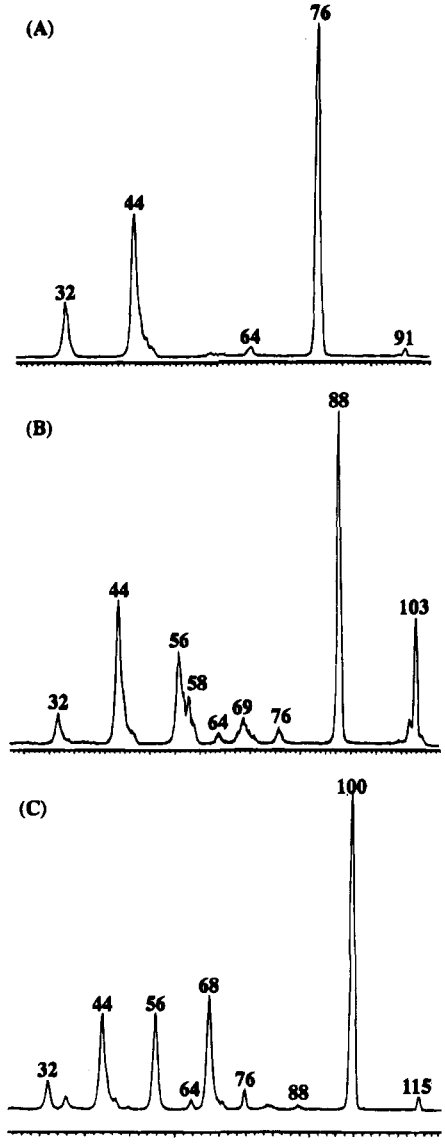

Figure 7. $NR(NH_3/O_2)$ mass spectra of methylated ions **b**−**d** [*m/z* 91 (A), *m/z* 103 (B), and *m/z* 115 (C)].

energy deposition in the ions during the reionization step.[27,28] The other difference is the charge-stripping peaks only barely seen in NRMS.[27] Because of the possibility of reionization of neutral molecules formed by fragmentation in the neutralization cell, the intensities of CS (*m/z* 44) and S (*m/z* 32) are often too high in the NR spectra (see Tables 4 and 5).[29]

The stability of ethenedithione (S=C=C=S, **6**) has been demonstrated previously by mass spectrometry as well as matrix isolation IR and UV spectroscopy.[1,30] Singlet ($^1\Delta_g$) and triplet ($^3\Sigma_g^-$) SCCS are calculated to lie close in energy, with the triplet 13 kJ mol^{-1} more stable than the singlet. However, MCSCF calculations slightly favor the singlet state.[30b,d] Higher level calculations are required in order to establish definitively the lowest energy state of ethenedithione. Both the singlet and triplet states of SCCS are predicted to be stable species in the gas phase (Table 2). Dissociation of singlet SCCS to CS + CS is endothermic (by 141 kJ mol^{-1}) and inhibited by an energy barrier of 178 kJ mol^{-1}. In agreement with experiments, loss of CS is calculated to be the lowest energy dissociation pathway for CS_2, C_2S_2, and C_3S_2 (Table 2). All SC_nS neutrals prefer a linear geometry, and the bonding between the carbons is cumulated rather than alternating triple and single bonds; the calculated C—C bond lengths are 1.280 Å (Figure 1).

$CH_3SC_nS^\bullet$ Radicals. $CH_3SCCS^\bullet$ is calculated to be a stable species in the gas phase, with the most favorable dissociation products ($CH_3^\bullet$ + SCCS) ca. 192 kJ mol^{-1} above the $CH_3SCCS^\bullet$ radicals. On the other hand, the even carbon systems (i.e. $CH_3SCS^\bullet$ and $CH_3SCCCS^\bullet$) are predicted to be unstable toward unimolecular fragmentation to $CH_3^\bullet$ + SC_nS (Table 2). Indeed, NR experiments (Figure 7) show a barely detectable recovery signal for $CH_3SCS^\bullet$ and $CH_3SCCCS^\bullet$. The base peaks of these spectra correspond to the reionization of S=C=S and S=C=C=C=S. In contrast, a significant recovery signal is observed in the NR mass spectrum of methylated ethenedithione ions (**c**) (Figure 7B), but they, too, decompose in part to SCCS neutrals.

Doubly-Charged Cations. For all the ions **b**−**g**, charge stripping is clearly observed in the $CA(O_2)$ spectra. Efficient charge-stripping processes during collisional activation have also been reported for polycarbon sulfide $C_nS^{\bullet+}$ and HC_nS^+ ions[27] and other cumulenes.[2,3,7,31] Consistent with the experimental findings, SC_nS^{2+} and $CH_3SC_nS^{\bullet 2+}$ dications are calculated to be stable species in the gas phase. The lowest energy fragmentation pathways for CS_2^{2+}, $C_2S_2^{2+}$, and $C_3S_2^{2+}$ are $CS^{\bullet+}$ + $S^{\bullet+}$ (endothermicity 105 kJ mol^{-1}), $CS^{\bullet+}$ + $CS^{\bullet+}$ (187 kJ mol^{-1}), and $CS^{\bullet+}$ + $C_2S^{\bullet+}$ (198 kJ mol^{-1}), respectively. The high stability of these doubly-charged ions may be rationalized in terms of their linear structures and charge distribution (charges

TABLE 6: Calculated Relative Stabilities[a,b] and Proton Affinities (298 K)[a] of *C*- and *S*-Protonated and -Methylated SC_nS

species	relative stability: protonation	relative stability: cationic methylation	proton affinity
SCS	102	53	686
SCCS	−76	−83	842
SCCCS	−69	−192	818

[a] QCISD(T)/6-311+G(2d,p) + ZPVE level. [b] *C*-Protonated/methylated species versus *S*-protonated/methylated species.

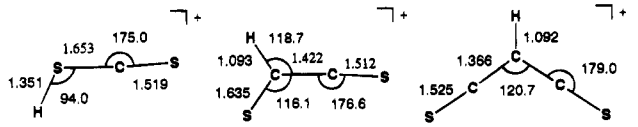

Figure 8. Optimized geometries (MP2/6-31G*) of protonated SC_nS; bond lengths in angstroms and bond angles in degrees.

localized mainly on the terminal H and S atoms), which minimize electrostatic repulsion between positive charges.[32]

Protonation of SC_nS. Protonation of SC_nS may occur on a carbon or a sulfur atom. The central carbon atom is calculated to be the most favorable site of protonation for carbon subsulfide, C_3S_2. The *S*-protonated form is 69 kJ mol^{-1} less stable than the *C*-protonated form. This result is consistent with the higher stability of the *C*-protonated form observed for the isoelectronic analogues, carbon suboxide[6] and iminopropadienones.[7] C_2S_2 also prefers a *C*-protonated form (Table 6). In contrast, carbon disulfide favors *S*-protonation rather than *C*-protonation. The preference for *C*-protonation of C_2S_2 and C_3S_2 may be attributed mainly to their charge distributions, which are negative on the carbon atoms. These theoretical preferences are in agreement with the experimental spectra as described below. We have determined the proton affinities (PA, 298 K) of CS_2, C_2S_2, and C_3S_2 at the QCISD(T)/6-311+G(2d,p) + ZPVE level (Table 6). The calculated proton affinity of CS_2 (686 kJ mol^{-1}) is in good agreement with the experimental value (694 kJ mol^{-1}).[33] This lends confidence to our predicted proton affinities for C_2S_2 and C_3S_2, 842 and 818 kJ mol^{-1} respectively. To facilitate future characterization of the protonated SC_nS ions (i.e. $HSCS^+$, $SCHCS^+$, and $SCCHCS^+$), we report their optimized (MP2/6-31G*) structures (Figure 8), vibrational frequencies (MP2/6-31G*), and rotational constants (Table 7). Although astronomical detection of linear CS_2, C_2S_2, and C_3S_2 is not straightforward, their protonated forms would be detectable by millimeter-wave spectroscopy.

The protonation of SC_nS was approached experimentally by chemical ionization methods, including FVP/CI/MS/MS. Protonation of CS_2 with methane (CH_5^+) results in a *m/z* 77 ion which fragments to give roughly equal intensities of *m/z* 44 (CS) and 45 (HCS or HSC), as well as ions of *m/z* 32 (S) and 33 (SH) (Figure 9A). The *S*-protonated structure $HSCS^+$ predicted by theory (vide supra) is in accord with this spectrum, and a strong signal for CS at *m/z* 44 would be difficult to rationalize for a *C*-protonated species.

Protonation of SCCS required FVP of **5** at 800 °C, followed by CI (CH_5^+) and CA mass spectroscopy. The spectrum (Figure 9B) suggests the *C*-protonated structure $SCHCS^+$ (**h**; major losses of S (to *m/z* 57) and CS (to *m/z* 45)).

C_3S_2 was similarly generated by FVP of the dithietane **3** at 750 °C followed by CI (CH_5^+) and CA mass spectroscopy. The spectrum (Figure 9C) suggests the *C*-protonated structure, $SCCHCS^+$ (**j**; *m/z* 101): the major fragments are due to loss of S (*m/z* 69) and CS (*m/z* 57). The same *m/z* 101 spectrum is obtained by $CA(O_2)$ of the molecular ion of the unsubstituted dithiolethione (**9**) (Figure 10). An MS/MS/MS experiment on the *m/z* 69 ions from **j** (generated from **9**) confirms the structure $HC{=}C{=}C{=}S^{\bullet+}$. The resulting spectrum was identical with that of $HC_3S^{\bullet+}$ from benzothiazole reported earlier.[27]

TABLE 7: Calculated Rotational Constants[a] (GHz), Vibrational Frequencies[b] (cm^{-1}), and Infrared Intensities (km mol^{-1}) of Protonated SC_nS

	$HSCS^+$	$SCHCS^+$	$SCCHCS^+$
	Rotational Constants		
A	283.79	27.631	17.218
B	3.0895	1.9803	1.1439
C	3.0562	1.8479	1.0726
	Vibrational Frequencies		
	2874 (430	3355 (28)	3350 (85)
	2556 (55)	3015 (24)	3010 (99)
	1496 (271)	1556 (87)	1728 (1773)
	914 (29)	1248 (25)	1644 (30)
	579 (10)	986 (6)	1216 (1)
	343 (8)	784 (30)	915 (0)
	303 (7)	761 (7)	798 (4)
		439 (11)	612 (38)
		331 (5)	493 (3)
		138 (10)	376 (0)
			346 (18)
			344 (3)
			88 (0)

[a] MP2/6-31G*-optimzied geometries. [b] MP2/6-31G* values, scaled by 0.9427 (ref 18).

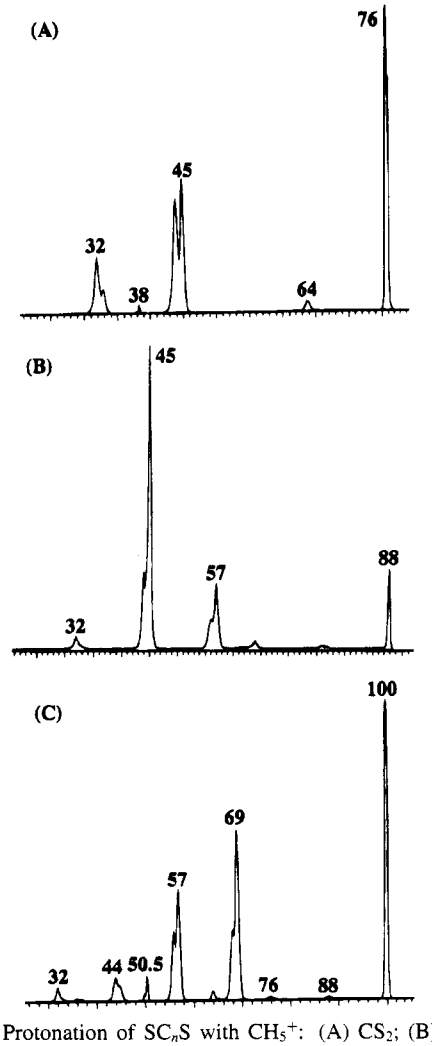

Figure 9. Protonation of SC_nS with CH_5^+: (A) CS_2; (B) C_2S_2; (C) C_3S_2. $CA(O_2)$ spectra.

Methylation of SC_nS. As with the protonation results, *S*-methylation is preferred for CS_2 but *C*-methylation for C_2S_2

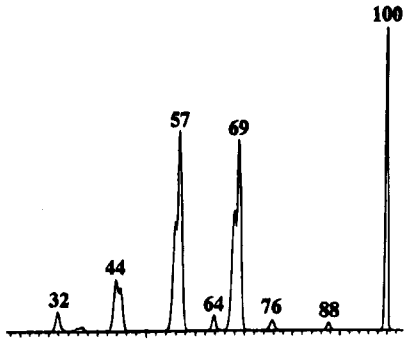

Figure 10. *C*-Protonated HC_3S_2 (**j**) for dithiolethione (**9**). CA(He) spectrum. When this spectrum is recorded with O_2 as the collision gas, the charge-stripping peak at *m/z* 50.5 is recovered (cf. Figure 9C).

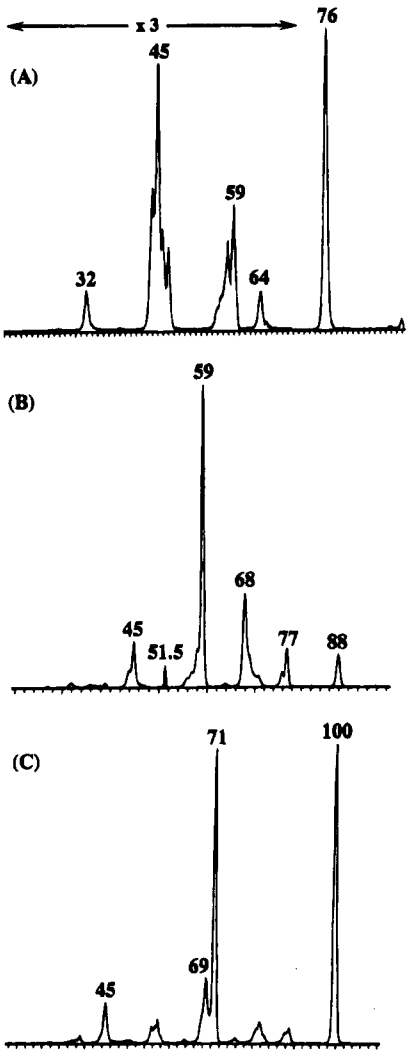

Figure 11. Methylation of SC_nS: (A) CS_2 (with CH_3Cl); (B) C_2S_2 (with CH_3Cl); (C) C_3S_2 (with CH_3I).

and C_3S_2. The calculated relative energies are given in Table 6, and the fragmentation patterns for the *C*-methylated ions in Table 3. The experimental spectra (Figure 11) were obtained by FVP of **5** and **3** as above (for production of C_2S_2 and C_3S_2, respectively), followed by cationic methylation using CH_3Cl or CH_3I, and CA mass spectroscopy. The result for CS_2 (Figure 11A) is essentially the same as in Figure 6A (i.e. *S*-methylation). However, the spectra obtained for C_2S_2 and C_3S_2 (Figure 11B and C) are dramatically different from those in Figure 6B and C, indicating that the thermodynamically more stable *C*-methylated ions (**i** and **k**) were formed in the CI processes. Theory also predicts that the fragmentation patterns of the *C*-methylated ions (Table 3) are significantly different from those of the *S*-methylated ions (Table 1). There is good accord between the calculated and experimental fragmentation patterns for ions **k** and **i** (Table 3, Figure 11), with the exception that we never observe the formation of CH_3^+ (*m/z* 15) even when this is calculated to be a facile process; this is a general phenomenon not limited to this study, and it is probably attributable to a discrimination against small masses by the detector dynode.

Further evidence allowing a differentiation of *S*- and *C*-methylated C_2S_2 was obtained by generation of bis(methylthio)-acetylene (**8**), which is obtained by FVP of the dithietane **3** (680 °C) as well as by FVP of the isoxazolone derivative **7**.[14] Loss of a methyl radical from the molecular ion of **8** gives CH_3-$SCCS^+$, identical with ion **c** described above. Further loss of $CH_3^\bullet$ gives $SCCS^{\bullet+}$, which by NR mass spectroscopy was shown to be identical with the previously generated C_2S_2 ions **f**.

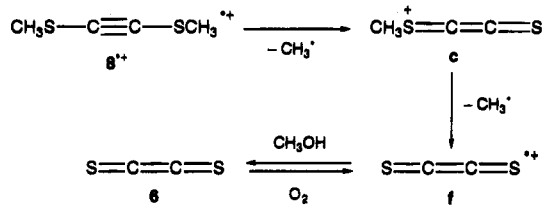

Conclusions

S-Methylated ions **b**–**d** are generated by dissociative ionization of **1**. A novel application of FVP/CI/MS/MS has allowed the production of *C*-protonated and *C*-methylated ions **h**–**k**. However, CS_2 is *S*-protonated and *S*-methylated under these conditions. Good agreement is observed between ab initio calculated and experimental stabilities and fragmentation patterns.

Acknowledgment. The Mons laboratory thanks the Fonds National de la Recherche Scientifique for its contribution toward the acqusition of the large-scale tandem mass spectrometer, VG AutoSpec 6F. The Brisbane laboratory thanks the Australian Research Council for financial support and for a research fellowship for M.W.W. The authors also thank Prof. Y. Mollier, University of Caen, France, for a gift of bis(methylthio)-1,2-dithiole-3-thione, and Prof. C. Th. Pedersen, Odense University, Denmark, for valuable discussions and samples of dithiolethiones.

References and Notes

(1) Wentrup, C.; Kambouris, P.; Evans, R. A.; Owen, D.; Macfarlane, G.; Chuche, J.; Pommelet, J. C.; Ben Cheikh, A.; Plisnier, M.; Flammang, R. *J. Am. Chem. Soc.* **1991**, *113*, 3130.

(2) Flammang, R.; Van Haverbeke, Y.; Laurent, S.; Barbieux-Flammang, M.; Wong, M. W.; Wentrup, C. *J. Phys. Chem.* **1994**, *98*, 5801.

(3) Flammang, R.; Landu, D.; Laurent, S.; Barbieux-Flammang, M.; Kappe, C. O.; Wong, M. W.; Wentrup, C. *J. Am. Chem. Soc.* **1994**, *116*, 2005.

(4) (a) Flammang, R.; Laurent, S.; Barbieux-Flammang, M.; Wentrup, C. *Rapid Commun. Mass Spectrom.* **1992**, *6*, 667. (b) Mosandl, T.; Stadtmüller, S.; Wong, M. W.; Wentrup, C. *J. Phys. Chem.* **1994**, *98*, 1080.

(5) Kappe, C. O.; Wong, M. W.; Moloney, D.; Flammang, R.; Wentrup, C. In preparation.

(6) Tortajada, J.; Provot, G.; Morizur, J. P.; Gal, J. F.; Maria, P. C.; Flammang, R.; Govaert, Y. *Int. J. Mass Spectrom. Ion Processes* **1995**, *141*, 241.

(7) Flammang, R.; Van Haverbeke, Y.; Wong, M. W.; Rühmann, A.; Wentrup, C. *J. Phys. Chem.* **1994**, *98*, 4814.

(8) For background information on the (so-far futile) efforts to generate O=C=C=O, see: (a) Berson, J. A.; Birney, D. M.; Dailey, W. P., III; Liebman, J. F. In *Modern Models of Bonding and Delocalization*; Liebman,

J. F., Greenberg, A., Eds.; VCH: New York, 1988; pp 391–441. (b) Sülzle, D.; Weiske, T.; Schwarz, H. *Int. J. Mass Spectrom. Ion Processes* **1993**, *125*, 75.

(9) Levsen, K.; Schwarz, H. *Angew. Chem., Int. Ed. Engl.* **1976**, *15*, 509.

(10) For reviews, see: (a) Wesdemiotis, C.; McLafferty, F. W. *Chem. Rev.* **1987**, *87*, 485. (b) Terlouw, J. K.; Schwarz, H. *Angew. Chem., Int. Ed. Engl.* **1987**, *26*, 805. (c) Holmes, J. L. *Mass Spectrom. Rev.* **1989**, *8*, 513. (d) McLafferty, F. W. *Science* **1990**, *247*, 925. (e) Plisnier, M.; Flammang, R. *Chim. Nouv.* **1990**, *8*, 893. (f) Goldberg, N.; Schwarz, H. *Acc. Chem. Res.* **1994**, *27*, 347.

(11) (a) Bateman, R. H.; Brown, J.; Lefevere, M.; Flammang, R.; Van Haverbeke, Y. *Int. J. Mass Spectrom. Ion Processes* **1992**, *115*, 205. (b) Brown, J.; Flammang, R.; Govaert, Y.; Plisnier, M.; Wentrup, C.; Van Haverbeke, Y. *Rapid Commun. Mass Spectrom.* **1992**, *6*, 249.

(12) Amzil, J.; Catel, J. M.; Lectostumer, G.; Mollier, Y.; Sauve, J. P. *Bull. Soc. Chim. Fr.* **1988**, 101.

(13) Kappe, C. O.; Pedersen, C. Th.; Catel, J. M.; Mollier, Y. *J. Chem. Soc., Perkin Trans. 2* **1994**, 351.

(14) (a) Cools, S. Mémoire de Licence, University of Mons-Hainaut, 1994. (b) Cools, S.; Flammang, R. To be published.

(15) Hehre, W. J.; Radom, L.; Schleyer, R. v. R.; Pople, J. A. *Ab Initio Molecular Orbital Theory*; Wiley: New York, 1986.

(16) Firsch, M. J.; Trucks, G. W.; Head-Gordon, M.; Gill, P. M. W.; Wong, M. W.; Foresman, J. B.; Johnson, B. G.; Schlegel, H. B.; Robb, M. A.; Replogle, E. S.; Gomperts, R.; Andres, J. L.; Raghavachari, K.; Binkley, J. S.; Gonzalez, C.; Martin, R. L.; Fox, D. J.; DeFrees, D. J.; Baker, J.; Stewart, J. J. P.; Pople, J. A. *GAUSSIAN 92*; Gaussian Inc.: Pittsburgh, PA, 1992.

(17) Pople, J. A.; Head-Gordon, M.; Raghavachari, K. *J. Chem. Phys.* **1987**, *87*, 5968.

(18) Pople, J. A.; Scott, A. P.; Wong, M. W.; Radom, L. *Isr. J. Chem.* **1993**, *33*, 345.

(19) Papavassiliou, G. C. *Chem. Scr.* **1985**, *25*, 167.

(20) Andreu, R.; Gayan, I.; Garin, J.; Orduna, J.; Saviron, M. *Org. Mass Spectrom.* **1994**, *29*, 321.

(21) Pedersen, C. Th. *Adv. Heterocycl. Chem.* **1982**, *31*, 63.

(22) Interestingly, a significant amount of $S_2^{\bullet+}$ (*m/z* 64) is present in all cases. However, these peaks are greatly reduced in the NR mass spectra (Table 5), thereby suggesting that $S_2^{\bullet+}$ arises from postcollisional isomerization.[7] Preliminary calculations at the MP2/6-31G* level indicate that there are stable $C_nSS^{\bullet+}$ and/or cyclic $SC_nS^{\bullet+}$ isomeric structures which may account for the formation of the $S_2^{\bullet+}$ ion. A recent study by Nagesha et al. has also suggested that bent $CS_2^{\bullet+}$ or CS_2^{2+} is responsible for the formation of $S_2^{\bullet+}$ from CS_2 by electron impact and fast collision.[23] It is worthwhile to note that the CA spectra of higher homologues of $C_3S_2^{\bullet+}$ do not show any $S_2^{\bullet+}$ ions.[24]

(23) Nagesha, K.; Bapat, B.; Marathe, V. R.; Krishnakumar, E. *Chem. Phys. Lett.* **1994**, *230*, 283.

(24) Süzle, D.; Beye, N.; Fanghänel, E.; Schwarz, H. *Chem. Ber.* **1990**, *123*, 2069.

(25) It is interesting to note that the preferred fragment products of the closed-shell $CH_3SC_nS^+$ ions are generally odd-electron radical cations and neutral radicals (Table 1). This is in sharp contrast to what would have been predicted from the so-called even-electron rule,[26] which states that even-electron cations should dissociate to even-electron daughter ions plus neutral fragments. Similar findings for the violation of the "even-electron rule" have been reported for a number of heterocumulene cations.[2,3,7,27] Our data for the $CH_3SC_nS^+$ ions further illustrate the almost total lack of adherence to the "rule".

(26) Karni, M.; Mandelbaum, A. *Org. Mass Spectrom.* **1980**, *15*, 53.

(27) Flammang, R.; Van Haverbeke, Y.; Wong, M. W.; Wentrup, C. *Rapid Commun. Mass Spectrom.* **1994**, *9*, 203.

(28) (a) Harnis, D.; Holmes, J. L. *Org. Mass Spectrom.* **1994**, *29*, 213. (b) Wiedmann, F. A.; Cai, J.; Westemiotis, C. *Rapid Commun. Mass Spectrom.* **1994**, *8*, 804.

(29) There is a small *m/z* 88 peak in the NRMS of $C_3S_2^{\bullet+}$ due to the loss of C: see note 23 in ref 27. See also Figure 5.

(30) (a) Sülzle, D.; Schwarz, H. *Angew. Chem., Int. Ed. Engl.* **1988**, *27*, 10. (b) Maier, G.; Reisenauer, H. P.; Schrot, J.; Janoschek, R. *Angew. Chem., Int. Ed. Engl.* **1990**, *29*, 1464. (c) Bohm, R. B.; Hannachi, Y.; Andrews, L. *J. Am. Chem. Soc.* **1992**, *114*, 6452. (d) Janoschek, R. *THEOCHEM* **1991**, *232*, 147.

(31) (a) Ast, T. *Adv. Mass Spectrom.* **1980**, *8A*, 555. (b) Rabrenovic, M. R.; Proctor, C. J.; Ast, T.; Herbert, C. G.; Brenton, A. G.; Beynon, J. H. *J. Phys. Chem.* **1983**, *87*, 3305. (c) Koch, W.; Macquin, F.; Stahl, D.; Schwarz, H. *Chimia* **1985**, *39*, 376. (d) Lammertsma, K.; Schleyer, P. v. R.; Schwarz, H. *Angew. Chem., Int. Ed. Engl.* **1989**, *28*, 132.

(32) For reviews, see: (a) Lammertsma, K.; Schleyer, P. v. R.; Schwarz, H. *Angew. Chem., Int. Ed. Engl.* **1989**, *28*, 132. (b) Radom, L.; Wong, M. W.; Gill, P. M. W. *Adv. Mass Spectrom.* **1989**, *11*, 702.

(33) Lias, S. G.; Liebman, J. F.; Levin, R. D. *J. Phys. Chem. Ref. Data* **1984**, *13*, 695.

JP951884P